

**K. Rokosz<sup>1a</sup>, T. Hryniewicz<sup>1b</sup>, W. Malorny<sup>2c</sup>**

<sup>1</sup> *Koszalin University of Technology, Faculty of Mechanical Engineering, Division of Surface Electrochemistry, Raclawicka 15-17, 75-620 Koszalin, Poland*

<sup>2</sup> *Hochschule Wismar-University of Applied Sciences Technology, Business and Design, Faculty of Engineering, DE 23966 Wismar, Germany*

<sup>a</sup>*rokosz@tu.koszalin.pl*, <sup>b</sup>*Tadeusz.Hryniewicz@tu.koszalin.pl*, <sup>c</sup>*frsimon@ipfdd.de*

## CHARACTERIZATION OF COATINGS CREATED ON SELECTED TITANIUM ALLOYS BY PLASMA ELECTROLYTIC OXIDATION

### ABSTRACT

The SEM and EDS results of coatings obtained on pure niobium and titanium alloys (NiTi and Ti6Al4V) by Plasma Electrolytic Oxidation in the electrolytes containing of 300 g and 600 g copper nitrate in 1 litre of concentrated phosphoric acid at 450 V for 3 minutes, are presented. The obtained coatings are porous and consist mainly of phosphorus within titanium and copper. For each coating, the Cu/P ratios were calculated. The maximum of that coefficient was found for niobium and Ti6Al4V alloy oxidised in the electrolyte containing 600 g of  $\text{Cu}(\text{NO}_3)_2$  in 1 dm<sup>3</sup> of  $\text{H}_3\text{PO}_4$  and equaling to 0.22 (wt%) | 0.11 (at%). The minimum of Cu/P ratio was recorded for NiTi and Ti6Al4V alloys oxidised by PEO in electrolyte consisting of 300 g of copper nitrate in 1 dm<sup>3</sup> of concentrated phosphoric acid and equals to 0.12 (wt%) | 0.06 (at%). The middle value of that ratio was recorded for NiTi and it equals to 0.16 (wt%) | 0.08 (at%).

**Keywords:** *Plasma Electrolytic Oxidation; PEO; Micro Arc Oxidation; MAO; SEM; Titanium alloy; NiTi*

### INTRODUCTION

Nowadays the electrochemical treatments, such as electropolishing (EP) [1-5], magneto-electropolishing (MEP) [6-13], high-current density electropolishing (HDEP) [14-15] as well as Plasma Electrolytic Oxidation (PEO) known also as Micro Arc Oxidation (MAO) [16-30] of biomaterial surfaces are very often used due to the biocompatibility effect. Most important is to fabricate the porous surface enriched in antibacterial elements such as silver and/or copper [30-35] with the least amount of toxic elements to the human body, such as vanadium, aluminum, and nickel [30, 36-43]. According to these requirements the best metallic biomaterials are metals such as titanium, niobium, zirconium, tantalum and their alloys [16-22]. However, till now the biomaterials such as titanium alloys, NiTi and Ti6Al4V, containing harmful

elements [24-30] are very popular and still used. Therefore, a new approach with novel technologies to eliminate the harmful elements are proposed and developed.

In the present paper, the Authors described the porous surfaces obtained on niobium biomaterial, and titanium alloys (NiTi, Ti6Al4V) after PEO processing in two electrolytes containing concentrated (85%) phosphoric acid and copper nitrate. A focus directed on the copper-to-phosphorus ratio in the porous coatings obtained.

## METHOD AND EXPERIMENTAL SET UP

The Plasma Electrolytic Oxidation experiments were performed on a set-up built in the cooperation with the Division of Applied Electronics and Electro-technology, Koszalin University of Technology (KUT), that was in details described in [27]. The PEO process was performed with the use of a constant voltage of 450 V. The electrolyte consisted of a concentrated 85% pure p.a.  $H_3PO_4$  (98 g/mole) acid, one liter, within 300 g and/or 600 g of  $Cu(NO_3)_2$ , consecutively. The pure niobium and NiTi, Ti6Al4V alloys of dimensions  $15 \times 20 \times 1$  mm, were prepared at the Faculty of Mechanical Engineering, KUT.

The scanning electron microscope Quanta 250 FEI with Low Vacuum and ESEM mode and a field emission cathode as well as the energy dispersive EDS system in a Noran System Six with nitrogen-free silicon drift detector, were employed. The magnification of 6000 times for SEM surface images and EDS analyses, was used.

## RESULTS

In Figures 1-2, the SEM images with EDS analyses of niobium after the PEO treatment at 450 V for 3 minutes, in the electrolyte consisting of 300 g  $Cu(NO_3)_2$  in 1 L  $H_3PO_4$ , are shown. The obtained surface is porous and consists of phosphorus, and niobium within copper. It should be noted that a part of niobium signal recorded by EDS may come from the matrix, that is improbable in the case of copper and phosphorus detected, which originate strictly from the electrolyte solution. That way, for the PEO coating characterization, the copper-to-phosphorus ratio will be used. In that case, the calculated  $Cu_{wt\%}/P_{wt\%}$  and  $Cu_{at\%}/P_{at\%}$  ratios are equal 0.16 and 0.08, respectively.

In Figures 3-4, the SEM images with EDS analyses of niobium after PEO treatment at 450 V for 3 minutes in the electrolyte consisting of 600 g  $Cu(NO_3)_2$  in 1 L  $H_3PO_4$ , are presented. Oxidation in the electrolyte within higher concentration of copper nitrate resulted in the formation of the porous coating with more developed surface. It should be also added that the coating is more porous with sharper edges than that one obtained in the solution with lower concentration (300 g) of copper nitrate. The copper-to-phosphorus  $Cu_{wt\%}/P_{wt\%}$  and  $Cu_{at\%}/P_{at\%}$  ratios for these surfaces are equal 0.22 and 0.11, respectively. This means that a higher concentration of copper nitrate in the solution results in obtaining a higher Cu/P ratio. However, the pore shapes may be crucial for the development of *e.g.* bone tissues, and that problem will be studied by the Authors in the near future.

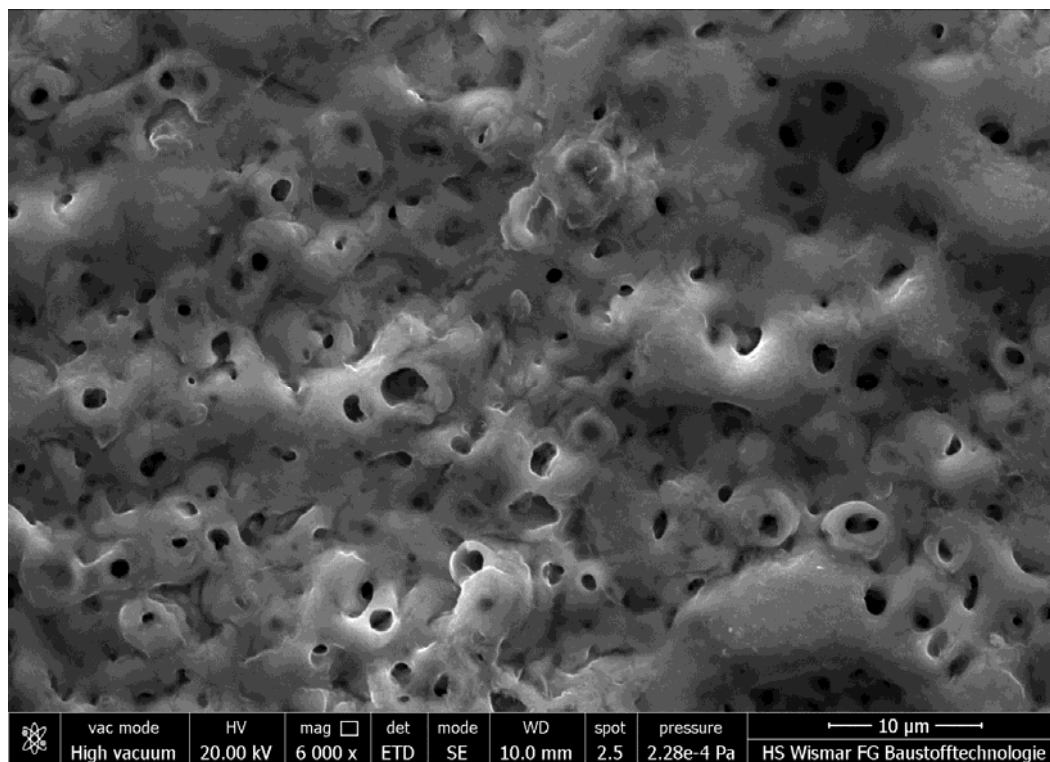


**Fig. 1.** SEM image of Niobium after PEO treatment at 450 V for 3 minutes in the electrolyte consisting of 300 g  $\text{Cu}(\text{NO}_3)_2$  in 1 L  $\text{H}_3\text{PO}_4$

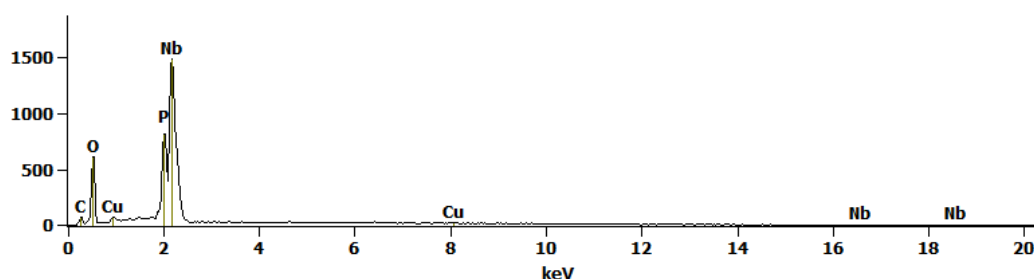


**Fig. 2.** EDS spectrum of Niobium after PEO treatment at 450 V for 3 minutes in the electrolyte consisting of 300 g  $\text{Cu}(\text{NO}_3)_2$  in 1 L  $\text{H}_3\text{PO}_4$  ( $\text{Cu wt\%/P wt\%} = 0.16$ ;  $\text{Cu at\%/P at\%} = 0.08$ )

In Figures 5-6, the SEM images with EDS analyses of NiTi alloy after PEO treatment at 450 V for 3 minutes, in the electrolyte consisting of 300 g  $\text{Cu}(\text{NO}_3)_2$  in 1 L ml  $\text{H}_3\text{PO}_4$ , are displayed. The obtained coating is porous and consists mainly of phosphorus, titanium within nickel and copper. It should be pointed out that a part of signals of titanium and nickel recorded by EDS may come from the substrate, that was described in details for niobium. Because both copper and phosphorus originate only from the electrolyte solution, the copper-to-phosphorus ratio will be used for the PEO coating characterization. The  $\text{Cu}_{\text{wt\%/P wt\%}}$  and  $\text{Cu}_{\text{at\%/P at\%}}$  ratios for that surface are equal 0.13 and 0.06, respectively. Additionally, it has to be pointed out that any cracks on the surface disqualify it as a coating on biomaterial. This is due to the possibility of further cracking of coating, resulting in its probable prompt destruction in case it is inducted into the human organism.

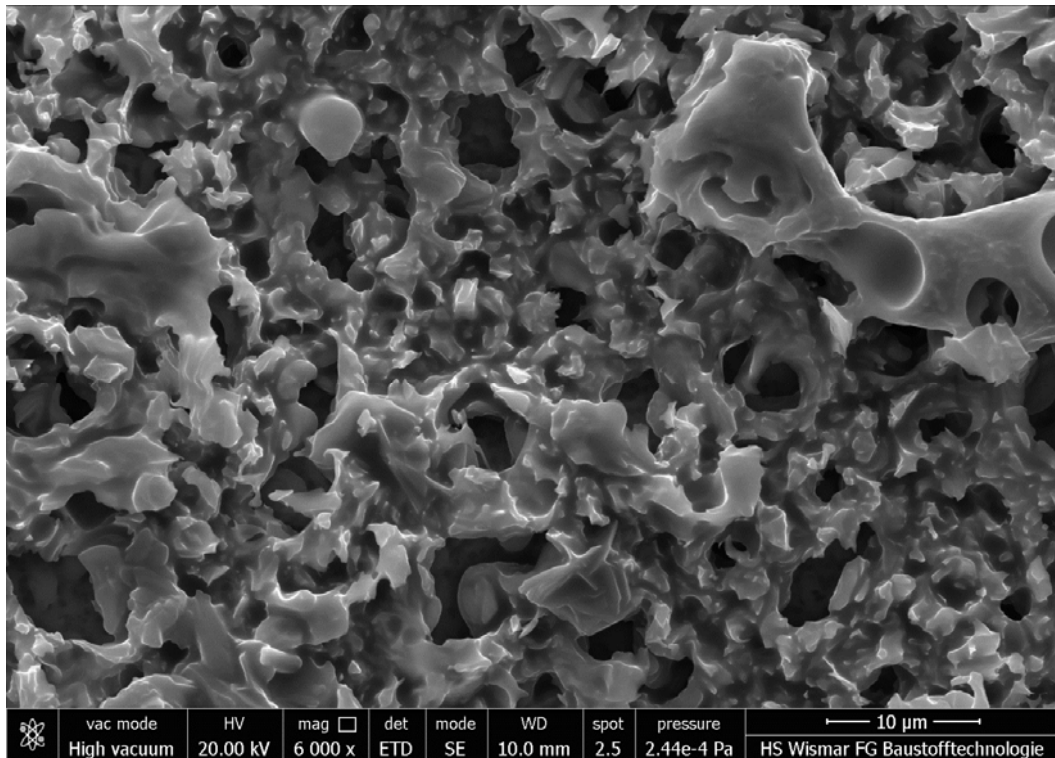


**Fig. 3.** SEM image of Niobium after PEO treatment at 450 V for 3 minutes in the electrolyte consisting of 600 g  $\text{Cu}(\text{NO}_3)_2$  in 1 L  $\text{H}_3\text{PO}_4$

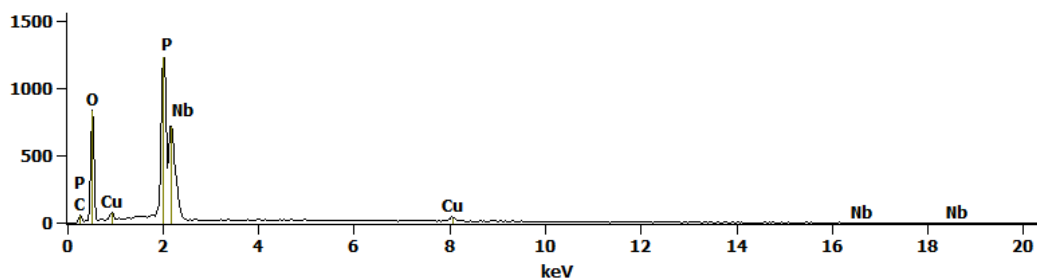


**Fig. 4.** EDS spectrum of Niobium after PEO treatment at 450 V for 3 minutes in the electrolyte consisting of 600 g  $\text{Cu}(\text{NO}_3)_2$  in 1 L  $\text{H}_3\text{PO}_4$  ( $\text{Cu wt\%/P wt\%} = 0.22$ ;  $\text{Cu at\%/P at\%} = 0.11$ )

In Figures 7-8, the SEM images with EDS analyses of Niti alloy after PEO treatment at 450 V for 3 minutes, in the electrolyte consisting of 600 g  $\text{Cu}(\text{NO}_3)_2$  in 1 L  $\text{H}_3\text{PO}_4$ , are presented. In that case the PEO coating has no trace of cracks and the surface development is similar to that one, obtained in the electrolyte within a lower amount of copper nitrate. Oxidation in the electrolyte within higher amount of copper nitrate resulted in the formation of porous coating with the copper-to-phosphorus  $\text{Cu}_{\text{wt\%}}/\text{P}_{\text{wt\%}}$  and  $\text{Cu}_{\text{at\%}}/\text{P}_{\text{at\%}}$  ratios being equal to 0.19 and 0.09, respectively. As it was in the case of niobium, the higher amount of copper nitrate in the electrolyte results in a higher Cu/P ratio.

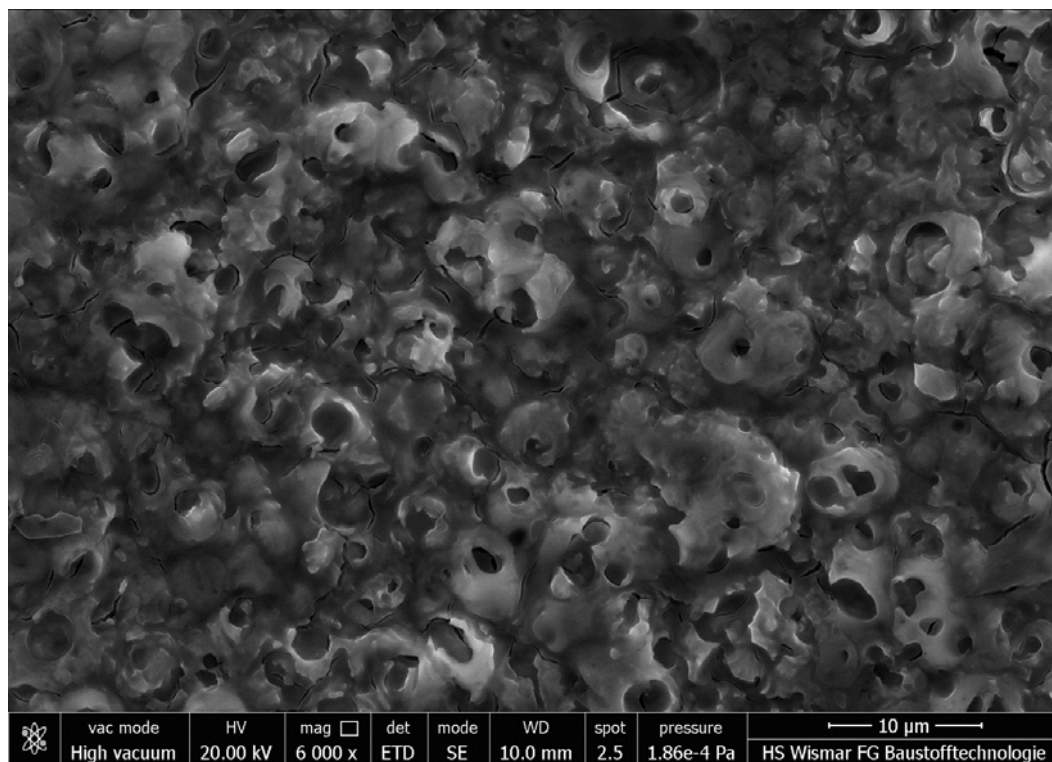


**Fig. 5.** SEM image of NiTi surface after PEO treatment at 450 V for 3 minutes in the electrolyte consisting of 300 g  $\text{Cu}(\text{NO}_3)_2$  in 1 L  $\text{H}_3\text{PO}_4$

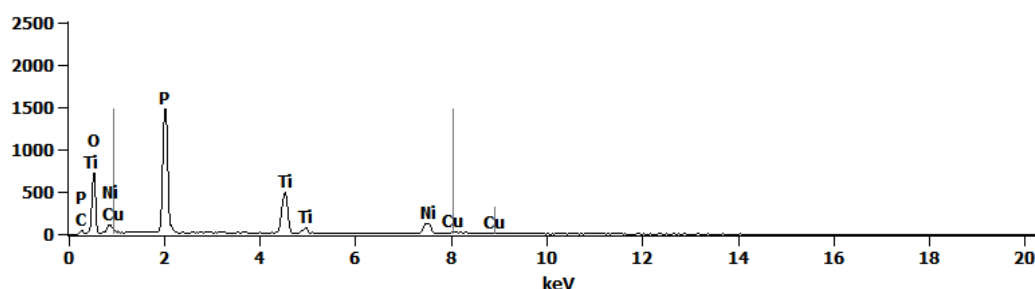


**Fig. 6.** EDS of NiTi surface after PEO treatment at 450 V for 3 minutes in the electrolyte consisting of 300 g  $\text{Cu}(\text{NO}_3)_2$  in 1 L  $\text{H}_3\text{PO}_4$  ( $\text{Cu wt\%/P wt\%} = 0.13$ ;  $\text{Cu at\%/P at\%} = 0.06$ )

In Figures 9-10, the SEM images with EDS analyses of Ti6Al4V alloy after the PEO treatment at 450 V for 3 minutes, in the electrolyte consisting of 300 g  $\text{Cu}(\text{NO}_3)_2$  in 1 L  $\text{H}_3\text{PO}_4$ , are shown. The obtained coating, similar as in the case of NiTi alloy, is porous, but with numerous cracks visible in the picture. It consists mainly of phosphorus, titanium within aluminium and copper. As it was in the case of NiTi alloy, the titanium and aluminium signals, which were recorded, may come from the substrate.

Copper and phosphorus, alike in all the cases described above, originate only from the electrolyte solution. The  $\text{Cu}_{\text{wt\%}}/\text{P}_{\text{wt\%}}$  and  $\text{Cu}_{\text{at\%}}/\text{P}_{\text{at\%}}$  ratios for that surface equal to 0.12 and 0.06, respectively. Additionally, it has to be noted that cracks on the surface may disqualify the coating due to the possibility of further cracking progress.

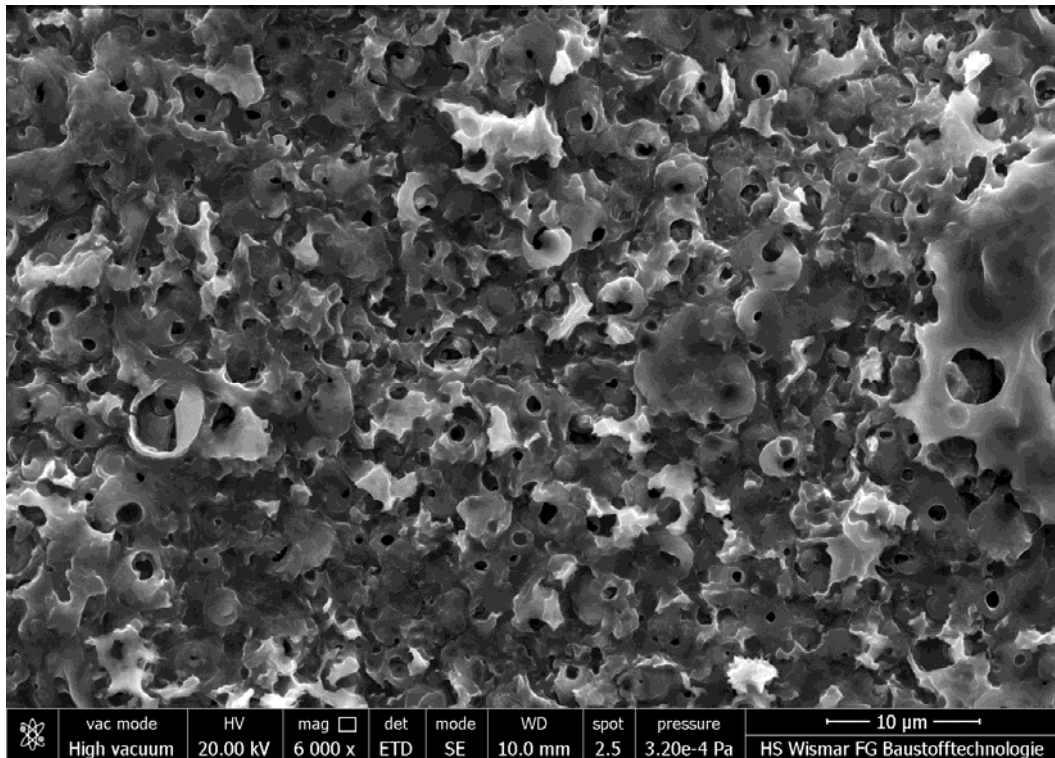


**Fig. 7.** SEM image of NiTi surface after PEO treatment at 450 V for 3 minutes in the electrolyte consisting of 600 g  $\text{Cu}(\text{NO}_3)_2$  in 1 L  $\text{H}_3\text{PO}_4$

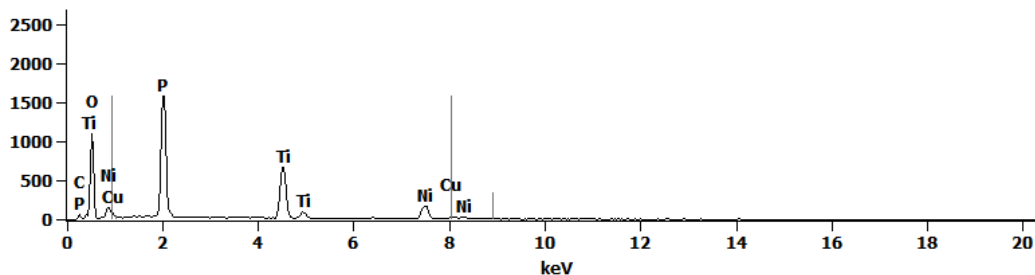


**Fig. 8.** EDS of NiTi surface after PEO treatment at 450 V for 3 minutes in the electrolyte consisting of 600 g  $\text{Cu}(\text{NO}_3)_2$  in 1 L  $\text{H}_3\text{PO}_4$  ( $\text{Cu wt\%/P wt\%} = 0.19$ ;  $\text{Cu at\%/P at\%} = 0.09$ )

In Figures 11-12, the SEM images with EDS analyses of Ti6Al4V alloy after PEO treatment at 450 V for 3 minutes, in the electrolyte consisting of 600 g  $\text{Cu}(\text{NO}_3)_2$  in 1 L  $\text{H}_3\text{PO}_4$ , are presented. The PEO coating is not cracked so that the surface development is proper and acceptable for further consideration. Oxidation in the electrolyte within higher concentration of copper nitrate resulted in the formation of the porous coating with the copper-to-phosphorus  $\text{Cu}_{\text{wt\%/P wt\%}}$  and  $\text{Cu}_{\text{at\%/P at\%}}$  ratios equal to 0.22 and 0.11, respectively. As it was in the case of niobium, the higher amount of copper nitrate in the electrolyte results in a higher Cu/P ratio.

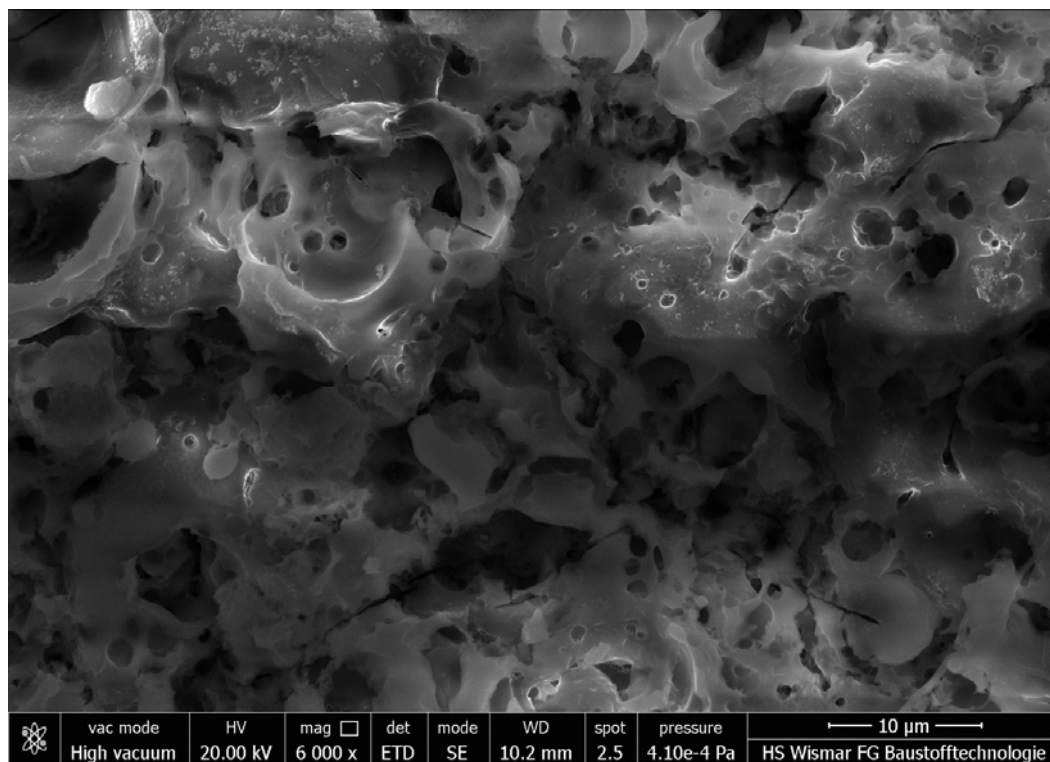


**Fig. 9.** SEM image of Ti6Al4V surface after PEO treatment at 450 V for 3 minutes in the electrolyte consisting of 300 g  $\text{Cu}(\text{NO}_3)_2$  in 1 L  $\text{H}_3\text{PO}_4$

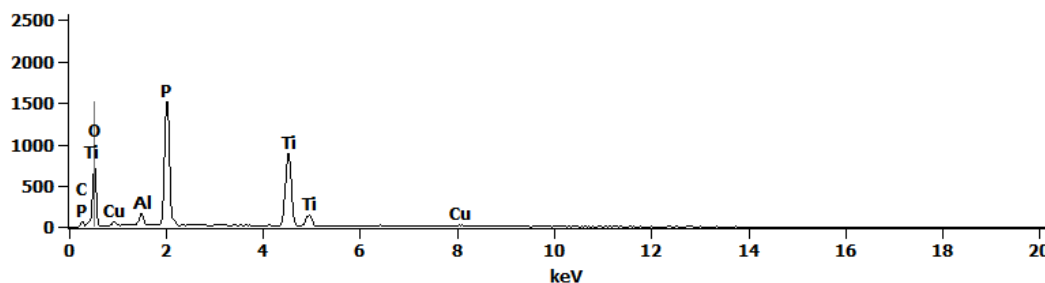


**Fig. 10.** EDS of Ti6Al4V surface after PEO treatment at 450 V for 3 minutes in the electrolyte consisting of 300 g  $\text{Cu}(\text{NO}_3)_2$  in 1 L  $\text{H}_3\text{PO}_4$  (Cu wt%/P wt% = 0.12; Cu at%/P at% = 0.06)

Figure 13 shows the copper-to-phosphorus ratio for biomaterials such as niobium and titanium alloys (NiTi, Ti6Al4V) oxidized in two electrolytes containing concentrated phosphoric acid within copper nitrate, by PEO treatment. It is clearly visible that the Cu/P ratio of copper, both taken for wt% as well as for at%, in that coefficient is always higher for the electrolyte solution with higher amount of copper nitrate inside. The maximum of that ratio was obtained for niobium and Ti6Al4V in the electrolyte containing 600 g of  $\text{Cu}(\text{NO}_3)_2$  in 1 L  $\text{H}_3\text{PO}_4$  and equals to 0.55 (wt%) and 0.11 (at%), respectively. The minimum was recorded for NiTi and Ti6Al4V oxidized by PEO in the electrolyte solution of 1 L  $\text{H}_3\text{PO}_4$  within 300 g of  $\text{Cu}(\text{NO}_3)_2$ .

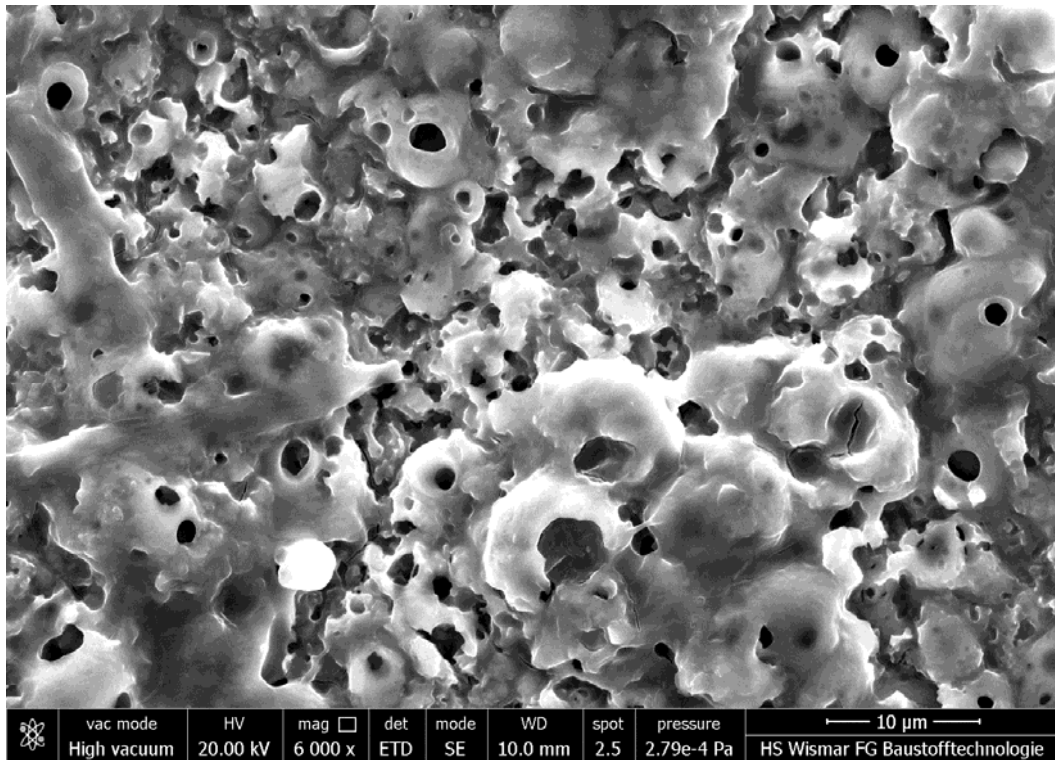


Fig. 11. SEM image of Ti6Al4V surface after PEO treatment at 450 V for 3 minutes in the electrolyte consisting of 600 g  $\text{Cu}(\text{NO}_3)_2$  in 1 L  $\text{H}_3\text{PO}_4$

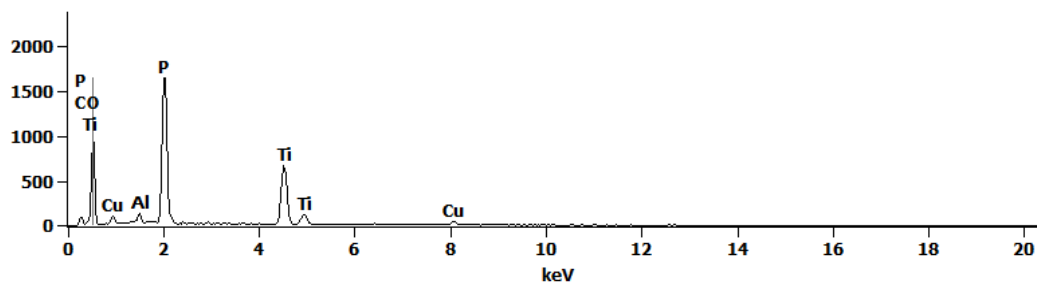


Fig. 12. EDS of Ti6Al4V surface after PEO treatment at 450 V for 3 minutes in the electrolyte consisting of 600 g  $\text{Cu}(\text{NO}_3)_2$  in 1 L  $\text{H}_3\text{PO}_4$  (Cu wt%/P wt% = 0.22; Cu at%/P at% = 0.11)

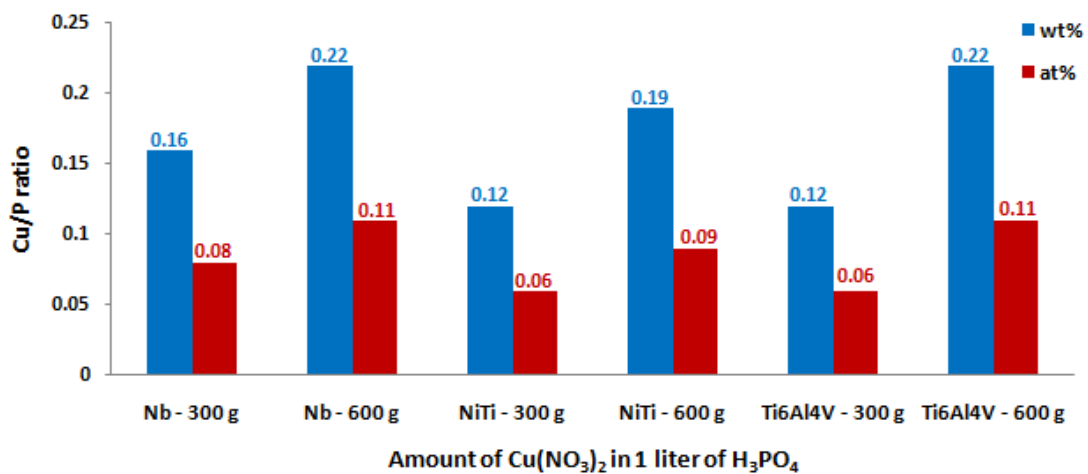


Fig. 12. Copper-to-Phosphorus ratio calculated on the basis of EDS analysis for selected biomaterials: Nb, NiTi, and Ti6Al4V

## CONCLUSIONS

In this paper, the results of the surface layers formed on selected biomaterials, such as niobium as well as titanium alloys (NiTi and Ti6Al4V) by PEO processing in the electrolytes containing of 300 g and 600 g copper nitrate in one litre of concentrated phosphoric acid, are given. The obtained results show that all the coatings are porous, however, the development and shapes of the created pores are different. Sharper pores were obtained on niobium after the PEO treatment at 450 V for 3 minutes in the electrolyte consisting of 600 g  $\text{Cu}(\text{NO}_3)_2$  in 1 L  $\text{H}_3\text{PO}_4$ . For all surfaces, the copper-to-phosphorus (Cu/P) ratios were calculated. The maximum of that coefficient was found for niobium and Ti6Al4V alloy oxidised in the electrolyte containing 600 g of  $\text{Cu}(\text{NO}_3)_2$  in 1 litre of  $\text{H}_3\text{PO}_4$  and equaling to 0.22 (wt%) | 0.11 (at%). The middle value of that ratio was recorded for NiTi and it equals to 0.16 (wt%) | 0.08 (at%). The minimum of Cu/P was recorded for NiTi and Ti6Al4V alloys oxidised by PEO in electrolyte consisting of 300 g of copper nitrate in 1 litre of concentrated phosphoric acid and equals to 0.12 (wt%) | 0.06 (at%).

Summing up, it should be noted that the research indicates that on all tested biomaterials the porous coatings after PEO treatment, in electrolyte containing phosphoric acid and copper nitrate, can be created. Because of an unknown reaction of human tissue on the obtained coatings, it is not possible to state clearly, which of the studied surfaces are the best due to the biocompatibility. For this purpose a biological studies should be carried out, performed by another team of researchers, that is to be done and presented under a separate paper.

## ACKNOWLEDGMENTS

Acknowledgments are sent to Prof. Frédéric Prima, Ecole Nationale Supérieure de Chimie de Paris, France, for the obtained TNZ samples used in this study.

## REFERENCES

1. Hryniewicz T., Physico-chemical and technological Fundamentals of electropolishing steels (Fizykochemiczne i technologiczne podstawy procesu elektropolerowania stali), 1989, Monograph no. 26, ed. by Koszalin University of Technology Publishing.
2. Hryniewicz T., On the surface treatment of metallic biomaterials (Wstęp do obróbki powierzchniowej biomateriałów metalowych), 2007, ed. by Koszalin University of Technology Publishing.
3. Rokosz K., Electrochemical Polishing in magnetic field (Polerowanie elektrochemiczne w polu magnetycznym), 2012, ed. by Koszalin University of Technology Publishing.
4. Hryniewicz T., Rokicki R., Rokosz K., Co-Cr alloy corrosion behaviour after electropolishing and "magneto-electropolishing" treatments, *Surface & Coatings Technology*, 62(17-18) (2008), 3073-3076.
5. Hryniewicz T., Rokosz K., Analysis of XPS results of AISI 316L SS electropolished and magneto-electropolished at varying conditions, *Surface & Coatings Technology*, 204(16-17) (2010), 2583-2592.

6. Hryniewicz T., Rokicki R., Rokosz K., Magneto-electropolishing for metal surface modification. *Transactions of The Institute of Metal Finishing*, 85(6) (2007), 325-332.
7. Hryniewicz T., Rokicki R., Rokosz K., Corrosion and surface characterization of titanium bio-material after magneto-electropolishing, *Surface & Coatings Technology*, 203(9)(2008), 1508-1515.
8. Hryniewicz T., Rokosz K., Polarization characteristics of magneto-electropolishing stainless steels, *Materials Chemistry and Physics*, 122(1) (2010), 169–174.
9. Rokosz K., Hryniewicz T., Raaen S., Characterization of passive film formed on AISI 316L stainless steel after magneto-electropolishing in a broad range of polarization parameters, *Journal of Iron and Steel Research*, 83(9) (2012), 910–918.
10. Hryniewicz T., Rokosz K., Investigation of selected surface properties of AISI 316L SS after magneto-electropolishing, *Materials Chemistry and Physics*, 123(1) (2010), 47–55.
11. Hryniewicz T., Rokosz K., Corrosion resistance of magneto-electropolished AISI 316L SS biomaterial, *Anti-Corrosion Methods and Materials*, 61(2) (2014), 57–64.
12. Hryniewicz T., Rokosz K., Valiček J., Rokicki R., Effect of magneto-electropolishing on nano-hardness and Young's modulus of titanium biomaterial, *Materials Letters*, 83 (2012), 69–72.
13. Hryniewicz T., Rokosz K., Rokicki R., Prima F., Nanoindentation and XPS Studies of Titanium TNZ Alloy after Electrochemical Polishing in a Magnetic Field, *Materials*, 8 (2015), 205-215.
14. Rokosz K., Hryniewicz T., Simon F., Rządkiwicz S., Comparative XPS analysis of passive layers composition formed on AISI 304L SS after standard and high-current density electropolishing, *Surface and Interface Analysis*, 47(1) (2015), 87–92.
15. Rokosz K., Lahtinen J., Hryniewicz T., Rządkiwicz S., XPS depth profiling analysis of passive surface layers formed on austenitic AISI 304L and AISI 316L SS after high-current-density electropolishing, *Surface & Coatings Technology*, 276 (2015), 516–520.
16. Simka W., Sadowski A., Warczak M., Iwaniak A., Dercz G., Michalska J., Maciej A., Modification of titanium oxide layer by calcium and phosphorus, *Electrochimica Acta*, 56(24) (2011), 8962-8968.
17. Jin F. Y., Tong H. H., Shen L. R., Wang K., Chu P. K., Micro-structural and Dielectric Properties of Porous TiO<sub>2</sub> Films Synthesized on Titanium Alloys by Micro-Arc Discharge Oxidation, *Materials Chemistry and Physics*, 100(1) (2006), 31-33.
18. Chung C.J., Su R.T., Chu H.J., Chen H.T., Tsou H.K., He J.L., Plasma electrolytic oxidation of titanium and improvement in osseointegration. *J. Biomed. Mater. Res. B Appl. Biomater.*, 101(6) (2013), 1023-1030.
19. Sowa M., Kazek-Kęsik A., Socha R.P., Dercz G., Michalska J., Simka W., Modification of tantalum surface via plasma electrolytic oxidation in silicate solutions, *Electrochimica Acta*, 114 (2013), 627-636.
20. Sowa M., Kazek-Kęsik A., Krząkała A., Socha R.P., Dercz G., Michalska J., Simka W., Modification of niobium surfaces using plasma electrolytic oxidation in silicate solutions, *Journal of Solid State Electrochemistry*, 18(11) (2014), 3129-3142.
21. Simka W., Sowa M., Socha R.P., Maciej A., Michalska J., Anodic oxidation of zirconium in silicate solutions, *Electrochimica Acta*, 104 (2013), 518-525.
22. Kazek-Kesik A., Krok-Borkowicz M., Jakobik-Kolon A., Pamula E., Simka W., Biofunctionalization of Ti-13Nb-13Zr alloy surface by plasma electrolytic oxidation. Part I, *Surface & Coatings Technology*, 276 (2015), 59-69.

23. Kazek-Kęsik A., Krok-Borkowicz M., Jakobik-Kolon A., Pamula E., Simka W., Biofunctionalization of Ti-13Nb-13Zr alloy surface by plasma electrolytic oxidation. Part II, *Surface & Coatings Technology*, 276 (2015), 23-30.
24. Simka W., Nawrat G., Chlode J., Maciej A., Winiarski A., Szade J., Radwanski K., Gazdowicz J., Electropolishing and anodic passivation of Ti6Al7Nb alloy, *Przemysł Chemiczny*, 90(1) (2011), 84-90.
25. Walsh F.C., Low C.T.J., Wood R.J.K., Stevens K.T., Archer J., Poeton A.R., Ryder Y. Plasma electrolytic oxidation (PEO) for production of anodised coatings on lightweight metal (Al, Mg, Ti) alloys, *Transactions of The Institute of Metal Finishing*, 87(3) (2009), 122-135.
26. Yerokhin A.L., Nie X., Leyland A., Matthews A. Characterisation of oxide films produced by plasma electrolytic oxidation of a Ti-6Al-4V alloy, *Surface & Coatings Technology*, 130(2-3) (2000), 195-206.
27. Rokosz K., Hryniewicz T., Dudek Ł., Malorny W., SEM and EDS analysis of NITINOL surfaces treated by Plasma Electrolytic Oxidation, *Advances in Materials Science*, 15(45) (2015), 41-47.
28. Rokosz K., Hryniewicz T., Plasma Electrolytic Oxidation as a modern method to form porous coatings enriched in phosphorus and copper on biomaterials, *World Scientific News*, 35 (2016), 44-61.
29. Rokosz K., Hryniewicz T., Raaen S., Development of plasma electrolytic oxidation for improved Ti6Al4V biomaterial surface properties, *The International Journal of Advanced Manufacturing Technology*, (2015), DOI: 10.1007/s00170-015-8086-y
30. Simka W., Habilitation summary of professional accomplishments (in Polish). Silesian University of Technology (Wydział Chemiczny, Politechnika Śląska), Gliwice, Chemical Engineering Department, 2013, 1-18.
31. Jelinek M., Kocourek T., Remsa J., Weiserová M., Jurek K., Mikšovský J., Strnad J., Galandáková A., Ulrichová J., Antibacterial, cytotoxicity and physical properties of laser-silver doped hydroxyapatite layers, *Materials Science and Engineering: C*, 33(3) (2013), 1242-1246.
32. Mishra G., Dash B., Pandey S., Mohanty P.P., Antibacterial actions of silver nanoparticles incorporated Zn-Al layered double hydroxide and its spinel, *Journal of Environmental Chemical Engineering*, 1(4) (2013), 1124-1130.
33. Rajendran A., Pattanayak D.K., Silver incorporated antibacterial, cell compatible and bioactive titania layer on Ti metal for biomedical applications, *RSC Advances*, 106(4) (2014), 61444-61455.
34. Trujillo N.A., Oldinski R.A., Ma H., Bryers J.D., Williams J.D., Popat K.C., Antibacterial effects of silver-doped hydroxyapatite thin films sputter deposited on titanium, *Materials Science and Engineering: C*, 32(8) (2012), 2135-2144.
35. Hempel F., Finke B., Zietz C., Bader R., Weltmann K-D., Polak M., Antimicrobial surface modification of titanium substrates by means of plasma immersion ion implantation and deposition of copper, *Surface and Coatings Technology*, 256 (2014), 52-58.
36. Bellows C.G., Heersche J.N., Aubin J.E., Aluminium accelerates osteoblastic differentiation but is cytotoxic in long-term rat calvaria cell cultures, *Calcif. Tissue Int.*, 65 (1999), 59-65.
37. Krewski D., Yokel R.A., Nieboer E., Borchelt D., Cohen J., Harry J., Kacew S., Lindsay J., Mahfouz A.M., Rondeau V., Human health risk assessment for aluminium, aluminium oxide, and aluminium hydroxide, *J. Toxicol. Environ. Health B Crit. Rev.*, 10(1) (2007), 1-269.
38. Solving Titanium Implant Osseointegration Problems by Using Epoxy/Carbon-Fiber-Reinforced Composite, *Titanium Today*, (2015), 26-28.

39. Browne R.C., Vanadium poisoning from gas turbines, *British Journal of Industrial Medicine*, 2(12) (1995), 57–59.
40. Jacobs J.J., Skipor A.K., Black J., Urban R., Galante J.O., Release and excretion of metal in patients who have a total hip-replacement component made of titanium-base alloy, *The Journal of Bone & Joint Surgery*, 73 (1991), 1475–1486.
41. Aluminum CAS # 7429-90-5, PUBLIC HEALTH STATEMENT, Agency for Toxic Substances and Disease Registry, Division of Toxicology and Environmental Medicine, <http://www.atsdr.cdc.gov>, Atlanta, 2008.
42. Landsberg J.P., McDonald B., Watt F., Absence of aluminium in neuritic plaque cores in Alzheimer's disease, *Nature*, 360 (1992), 65–68.
43. Seiler H.G., Sigel H., Sigel A., *Handbook of toxicity of inorganic compounds*, Marcel Dekker Inc., 1998, New York, NY.